



## Analysis Structure and Morphology of Bentonite-Opba Nanocomposites as Nanofillers

Erna Frida<sup>a</sup> • Nurdin Bukit<sup>b\*</sup> • Ferry Rahmat Astianta Bukit<sup>c</sup> • Bunga Fisikanta Bukit<sup>d</sup>

<sup>a</sup>Department of physics Universitas Sumatera Utara, 20155, Medan, Indonesia

<sup>b</sup>Department of physics, Universitas Negeri Medan, 2022, Medan, Indonesia

<sup>c</sup>Department of Electrical Engineering, Universitas Sumatera Utara, 20155, Medan, Indonesia

<sup>d</sup>Universitas Quality Berastagi, 22153, Berastagi, Indonesia

Received 07 19 2021; accepted 10 04 2021

Available 04 30 2022

**Abstract:** This study aims to analyze the structure and morphology of bentonite-OPBA nanocomposite used as a nanofiller. The methods used to synthesis bentonite nanoparticles are ball mill and co-precipitation and modification with surfactant cetyltrimethylammonium bromide (CTAB). Likewise, the OPBA synthesis process with the ball mill process and co-precipitation. Characterization using X-ray diffraction (XRD), Fourier transform infrared spectroscopy (FTIR), scanning electron microscope (SEM), FTIR and X-ray fluorescence (XRF). The results of characterization using XRD showed a decrease in particle size in bentonite-OPBA nanocomposites. The peak angle  $2\theta$  are 19.97°, 26.43°, 35.29°. After being modified with CTAB surfactant, there was a shift in peak, which indicated CTAB had been inserted into the layer of Na-bentonite by ion exchange. The SEM results show uniformity of particle size in Bentonite-OPBA nanocomposite. Meanwhile, the FTIR results showed absorption peaks indicating bonding in the nanocomposite, confirmed by XRF results. The XRF results show the content of SiO<sub>2</sub> and Al<sub>2</sub>O<sub>3</sub> in the nanocomposite so that it can be applied as a nanofiller.

**Keywords:** Nanoparticles, CTAB, Geopolymer

\*Corresponding author.

E-mail address: [nurdinbukit5@gmail.com](mailto:nurdinbukit5@gmail.com) (Nurdin Bukit).

Peer Review under the responsibility of Universidad Nacional Autónoma de México.

## 1. Introduction

Bentonite is an abundant natural resource in Indonesia, but its utilization has not been optimal. Bentonite is a layered silicate clay mineral consists of Montmorillonite with a d value of about 1 nm. It can be incorporated or Intercalated with many guest species, thus providing a wide range of possibilities for its wide application in composites (Wang et al., 2014). Bentonite has hydrophilic properties, so it is not compatible with most polymer materials. Therefore, chemical modifications must be carried out to make the surface more hydrophobic. (Fisli & Yusuf, 2010; Ginting et al., 2017; Rabiatal et al., 2020). Acid washing with various solutions, including HCl, H<sub>2</sub>SO<sub>4</sub> and HNO<sub>3</sub> (Abeywardena et al., 2017; Sirait et al., 2018, 2017) and intercalation with cationic surfactants are useful for modifying bentonite. One of the cationic surfactants is CTAB (cetyltrimethylammonium bromide) or HDTMA (Hexadecyltrimethyl ammonium bromide). Activation with acid has two effects: first is removing exchangeable cations such as Na<sup>+</sup> and Ca<sup>2+</sup> with protons from the activating acid, and the second is removing cations such as Al<sup>3+</sup> (dealumination), Mg<sup>2+</sup> and Fe<sup>2+</sup>. (Ogunlaja & Pal, 2020).

Bentonite is currently studied as a nanofiller in nanocomposites (Bukit & Frida, 2013; Ginting et al., 2017; Majid et al., 2020). The addition of bentonite as a nanofiller can improve the properties of thermal resistance, mechanical properties, chemical resistance and flammability of nanocomposites (Sirait et al., 2017, 2018; Rihayat et al., 2019).

Nanofillers will tend to form agglomerations when inserted into the polymer matrix. Therefore, the incorporation of nanofillers is required to integrate different functional groups, which facilitates homogeneous dispersion. Silica nanoparticles are the most preferred nanofillers over metal and metal oxide nanoparticles as a reinforcing phase in advanced composite materials. (Alexandre & Dubois, 2000; Karnati et al., 2020). Previous studies have carried out the incorporation of bentonite and silica nanoparticles. The addition of nano bentonite/nano-silica to the Phenol novolac epoxy resin overcomes the resin's structural brittleness and improves mechanical properties (Ahmadi, 2020). Furthermore, the super-tough properties of Hydrogel with the addition of Bentonite/SiO<sub>2</sub> nanocomposite (Yu et al., 2018)

Plantation waste such as Oil Palm Boiler Ash (OPBA) contains silica. OPBA is biomass with silica content that has the potential to be utilized. The content of OPBA consists of SiO<sub>2</sub>, Al<sub>2</sub>O<sub>3</sub>, Fe<sub>2</sub>O<sub>3</sub>. (Bukit et al., 2019; Ginting, Bukit, Frida, et al., 2020). Currently, the use of OPBA is not optimal, where most of the OPBA waste causes many environmental problems (Hamada et al., 2018). The original OPBA has a large particle size with a porous texture. The crushing and grinding process will obtain smaller OPBA particles. In addition, the grinding process will increase the fineness of OPBA particles and

specific gravity. OPBA applications in previous studies include adsorbent, filler, pozzolan, mortar, and cement paste (Bukit et al., 2020; Bukit et al., 2018; Ginting et al., 2018; Ginting, Bukit, Motlan, et al., 2020; Ismail et al., 2015; Saba et al., 2015).

Ball mill, coprecipitation, and addition of CTAB surfactant are methods used in bentonite preparation. While the extraction of silica from OPBA through the ball mill and coprecipitation process. Furthermore, the incorporation of palm oil boiler ash into bentonite was carried out using the facile method.

## 2. Materials and methods

The materials used for this study are sodium bentonite, OPBA from PT. DPI (Dhajaja Putra Indonesia) Asahan District North Sumatra Indonesia, 7M HCl, 7M NaOH, NH<sub>4</sub>OH Merck Pro Analis, CTAB from Himedia AR Grade.

### 2.1. Synthesis of bentonite nanoparticle

Bentonite was calcined at 700°C for 5 hours and milled with a Planetary Ball Mill type ball mill for 10 hours. Then, bentonite was synthesized by the coprecipitation method using 7M HCl as a solvent and 7M NaOH as a precipitate. Bentonite was modified by adding CTAB. CTAB solution and bentonite dispersion were mixed at 70°C for 3 hours and then filtered. The mixture was then dried in an oven at 150°C for 2 hours. The schematic of the nano bentonite synthesis is shown in Figure 1.

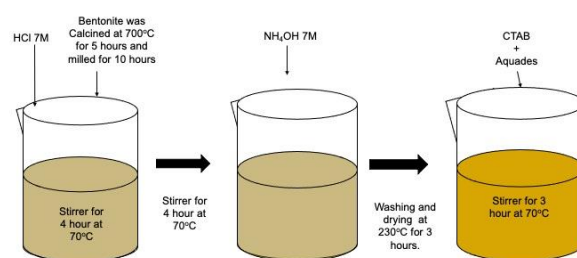


Figure 1. Bentonite Nanoparticle Synthesis Scheme.

### 2.2. Synthesis of OPBA nanoparticle

OPBA obtained from palm oil mill waste was dried in an oven for 2 hours at a temperature of 250°C. Furthermore, OPBA was calcined and ground with a ball mill type Planetary Ball Mill type Retsch PM200 for 10 hours with a rotation of 250 rpm. Coprecipitation was carried out using 7M HCl as a solvent and NH<sub>4</sub>OH as a precipitate. OPBA was washed with distilled water to produce a neutral pH. Then, it was dried in an oven at a temperature of 230°C for 2 hours. The schematic of the synthesis of OPBA Nanoparticles is shown in Figure 2.

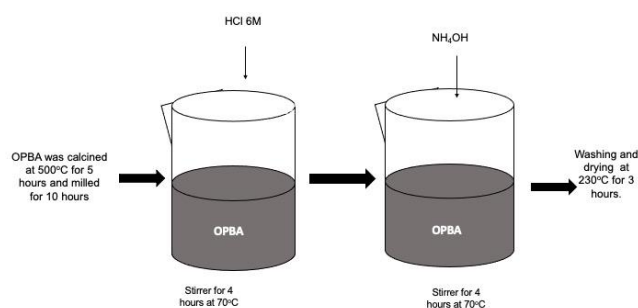


Figure 2. The Schematic of Synthesis OPBA Nanoparticle.

### 2.3. Synthesis of bentonit – OPBA nanocomposite

The nanocomposite synthesis process was carried out by mixing Btbc-CTAB and OPBA-BC and adding 100 ml of absolute ethanol using a stirrer at 70°C for 2 hours. Then filtered and dried at 150°C for 2 hours. Table 1 shows the label of each sample.

Table 1. Sample label.

Label	Description
Btb	Calcined and ball milled bentonite
Btbc	Bentonite calcined and ball mill and co-precipitation
Btbc-CTAB	Calcined bentonite, ball mill, co-precipitation and modification with CTAB
OBBA-B	Calcined and ball milled OPBA
OPBA-BC	OPBA calcined, ball mill and co-precipitation
Bentonit-OPBA	Bentonite calcined, ball mill, co-precipitation process and modification with CTAB mixed with OPBA calcined and ball mill and co-precipitation.

## 3. Result

### 3.1. X-ray diffraction (XRD) analysis

Analysis of X-ray diffraction (XRD) on the sample using a Goniometer type Shimadzu 6000 instrument with a Cu/Kα1 X-ray source with a wavelength, = 1.54056. The analysis was carried out with an angle of 2θ starting from 10° to 70°. The diffractogram is compared with the JCPDS (Joint Committee on Powder Diffraction Standard) database to identify the diffraction pattern of the synthesized material. Figure 3 shows

the XRD diffraction pattern of the sample. Meanwhile, Table 3 shows the data on the physical and structural properties of the sample determination of the crystal size of the material using the Scherrer equation:

$$D = \frac{K\lambda}{\beta \cos \theta} \quad (1)$$

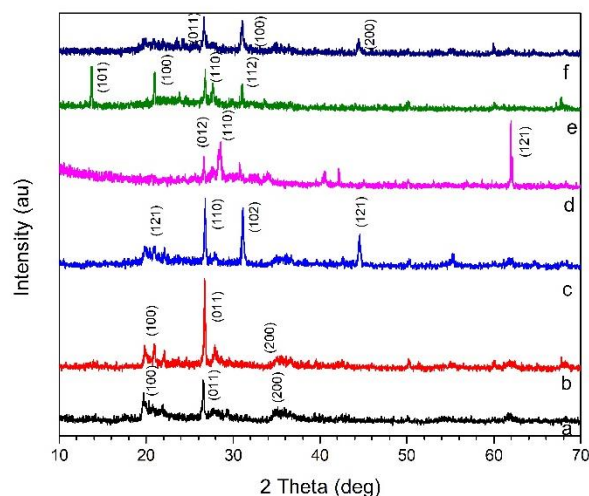


Figure 3. X-ray diffraction of (a) Btb, (b) Btbc, (c) Btbc-CTAB, (d) OPBA-B, (e) OPBA-BC, (f) Nanocomposite Bentonit-OPBA.

Where D is the crystal size (Å), λ is the X-ray wavelength used with CuK Cu radiation (λ = 1.54056), θ is the Bragg angle, κ is Scherrer's constant has a general value of 0.9 and β is the half-peak width of Full Width at Half Maximum (FWHM) in radians. By using the Scherrer equation and processing data with Origin software, the particle size obtained is shown in Table 2.

Table 2. Nanoparticle size from XRD analysis.

Sample	D (nm)
Btb	24.79
Btbc	15.52
Btbc-CTAB	18.06
OPBA-B	53.56
OPBA-BC	34.59
Nanocomposite Bentonit-OPBA	18.96

The increasing of particle size in Btbc-CTAB is due to CTAB acting as an ion exchanger with hydrated cations localized in the bentonite interlayer space and promoted rearrangement of the clay layer. So that, the structure of the material obtained is very regular and sharp reflection peaks. In other words, CTAB has small bentonite particles are assembled into larger

particles with an orderly structure because of the relationship between CTAB particles with small negatively charged edges bentonite particles (My Linh et al., 2020). Meanwhile, in Bentonite-OPBA Nanocomposite, there was a decrease in particle size. This decrease shows that bentonite can inhibit the growth of OPBA (Wang et al., 2020). The peak angle Btb, Btbc occurs at an angle of  $2\theta$  are  $19.97^\circ, 26.43^\circ, 35.29^\circ$ . After modification with CTAB surfactant peak shift occurs, which indicated CTAB had been inserted into the layer of Na-bentonite by ion exchange. Alkylammonium ions intercalated between the layers of raw bentonite resulting in enhanced basal spacing (Andrunik & Bajda, 2019; Yuzhen et al., 2020). Meanwhile, in figures 3d and 3e, the  $2\theta$  is around  $26.7^\circ$ . High-intensity peaks were observed, indicating silica content, the main crystalline component in OPBA nanoparticles (Abdullah et al., 2021; Liang et al., 2019).

### 3.2. Scanning electron microscopy (SEM) analysis

To describe the surface morphology of Bentonite-OPBA, SEM analysis was carried out using the EVO MA 10 Zeiss instrument. SEM of the sample are presented in Figure 4.

Figure 4 show a smooth and irregular appearance, and Btb presents scattered and different sizes beam structures. However, the surface rough modified bentonite morphology and was accompanied by a small number of holes and robust areas (Chen et al., 2020; Justice Babu et al., 2018; Siva et al., 2018). At the same time, SEM image of Btbc-CTAB showing crimp, edges morphology and small pieces of Btb form block structure (Wang et al., 2020). Meanwhile, Figure 4f shows a change in the morphology. Morphology looks more uniform than the other samples. These changes indicate that the synthesis of bentonite-OPBA nanocomposite can produce optimal morphology.

Table 3. XRD Analysis of OPBA and Bentonit Nanoparticles.

Date	Btb	Btbc	Btbc-CTAB	OPBA-B	OPBA-BC	Nanocomposite Bentonit-OPBA
Crystal system	trigonal (hexagonal axes)	trigonal (hexagonal axes)	trigonal (hexagonal axes)	trigonal (hexagonal axes)	trigonal (hexagonal axes)	trigonal (hexagonal axes)
Space group	P 32 2 1 (154)	P 32 2 1 (154)	P 32 2 1 S	P 32 2 1(154)	P 32 2 1 S	P 31 2 1 (152)
Unit cell	a=4.9180 Å c=5.4070 Å	a=4.9180 Å c=5.4070 Å	a= 4.9290 Å c= 5.3190 Å	a= 4.9124 Å c= 5.4039 Å	a= 4.9180 Å c= 5.4070 Å	a=4.6764 Å c=5.2475 Å
Density	2.64100 g/cm <sup>3</sup>	2.64100 g/cm <sup>3</sup>	2.675 g/cm <sup>3</sup>	2.6490g/cm <sup>3</sup>	2.643 g/cm <sup>3</sup>	3.01200 g/cm <sup>3</sup>
2 theta angle	26.43	26.71	26.79	61.95	13.67	26.71
Maximum d <sub>hkl</sub>	011	011	(110)	121	101	011
Intensity I/I <sub>0</sub>	1000	1000	1000	1000	1000	1000
Lattice distance d (Å)	3.3458	3.2061	3.3273	1.4965	6.4790	3.2061
2 theta angle	19.97	19.97	31.14	28.55	20.92	30.95
Maximum d <sub>hkl</sub>	100	100	102	012	100	100
Intensity I/I <sub>0</sub>	893.4	893.4	997.59	4902	798.52	858.2
Lattice distance d (Å)	4.2591	4.2591	2.8718	3.1255	4.2460	4.0499
2 theta angle	35.29	35.29	44.50	26.65	26.74	44.43
Maximum d <sub>hkl</sub>	200	2 0 0	121	110	110	200
Intensity I/I <sub>0</sub>	484.1	484.1	466.48	2867	766.94	527.3
Lattice distance d (Å)	2.1296	2.1296	2.0360	3.3440	3.3341	2.0249
2 theta angle	-	-	19.86	-	30.98	-
Maximum d <sub>hkl</sub>	-	-	121	-	112	-
Intensity I/I <sub>0</sub>	-	-	249.48	-	504.51	-
Lattice distance d (Å)	-	-	4.4711	-	2.8862	-

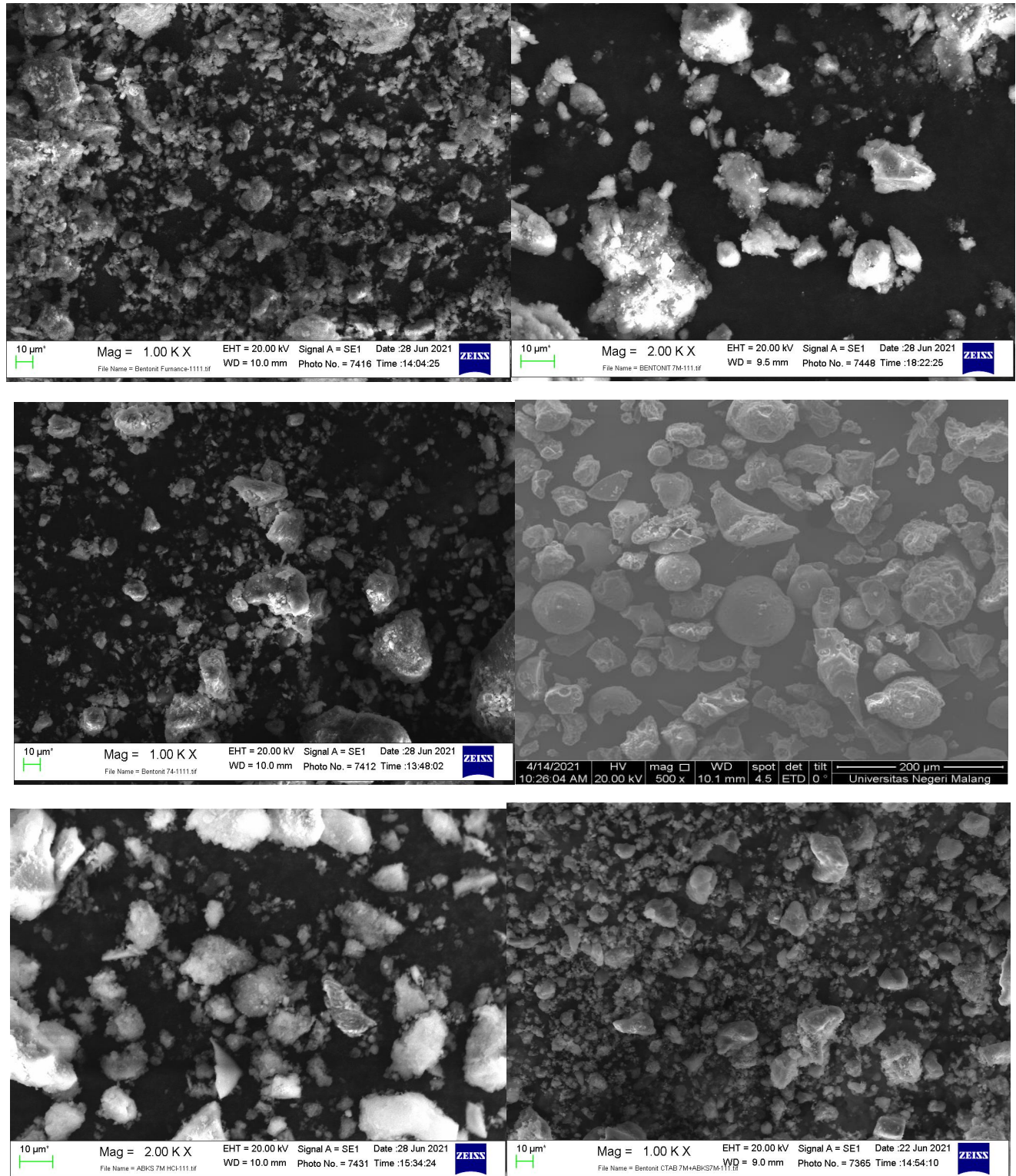


Figure 4. Scanning Electron Microscopy of (a) Btb, (b) Btbc, (c) Btbc-CTAB, (d) OPBA-B, (e) OPBA-BC, (f) Nanocomposite Bentonit-OPBA.

### 3.3. Fourier transform infrared (FTIR) analysis

Analysis of functional groups in the sample was carried out using the FTIR Shimadzu model IR-Prestige-21 made in Japan with Resolution = 4.0. Wavenumber range from 500 cm<sup>-1</sup> to 4000 cm<sup>-1</sup>. The FTIR graph is presented in Figure 5.

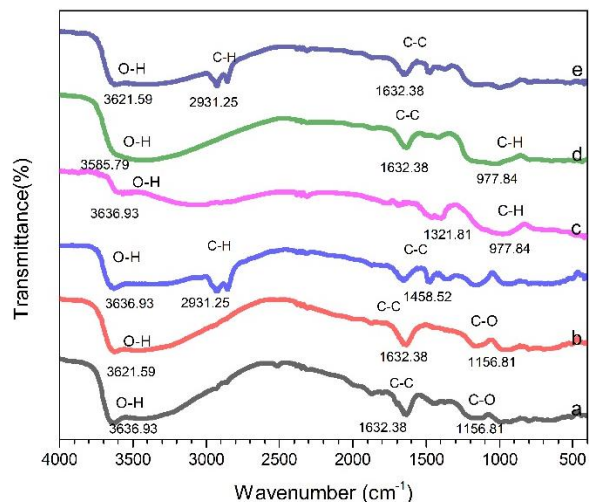


Figure 5. FTIR Graph of (a) Btb, (b) Btbc, (c) Btbc-CTAB, (d) OPBA-B, (e) OPBA-BC, (f) Nanocomposite Bentonit-OPBA.

From Figures 5a and 5b, it can be seen that the absorption peaks are almost similar. The presence of a Signal peak at 1632.38 cm<sup>-1</sup> corresponds to the deformation of H<sub>2</sub>O (adsorbed between the aluminum-silicate layers). The band at 3630 cm<sup>-1</sup> is associated with the stretching of Al-OH (Jenita Rani et al., 2017; Legarto et al., 2019; Shakir et al., 2018).

However, in Figure 5c new absorption peaks appear at 1458.52 and 2931.25. These peaks indicate that the CTAB molecules were intercalated between the bentonite mineral layers and the higher intensity of the characteristic of modified bentonite peaks compared with that in natural bentonite, indicating the organophilic nature of the modified bentonite.

FTIR Showed that CTAB had achieved surface modification of natural bentonite (Ibrahim & Abd Ali, 2020). Figures 5d and 5e show the absorption peak at 977.84. The absorption band at 981.33 cm<sup>-1</sup> indicates that the increase in silica strengthening has increased in the polymerization process. In figure 5d, the absorption peak of 2931.25 which is owned by CTAB reappears (Schampera et al., 2016). This peak indicates the success in the synthesis of Bentonite-OPBA nanocomposite.

### 3.4. X-ray fluorescence (XRF) analysis

The chemical composition was determined by XRF analysis. Table 4 shows SiO<sub>2</sub> and Al<sub>2</sub>O<sub>3</sub> as the most common compounds found in Btb, Btbc, Btbc-CTAB, Bentonite-OPBA Nanocomposite (Akl et al., 2013; Dhawale et al., 2018; Zarina et al., 2013). Since the amount of SiO<sub>2</sub> and Al<sub>2</sub>O<sub>3</sub> in boiler ash is 49%, this material can be used as a geopolymer.

The CaO content was the second-highest that has been reported to affect the mixed properties of the fresh geopolymer and the hardened geopolymer. In addition, the Si/Al ratio plays a vital role in determining geopolymeric applications in industry (Jaarsveld et al., 2004).

Table 4. Elements obtained from XRF analysis.

Compound	Btb (wt%)	Btbc (wt%)	Btbc-CTAB (wt%)	OPBA-B (wt%)	OPBA-BC (wt%)	Nanocomposite Bentonit-OPBA (wt%)
SiO <sub>2</sub>	59.3	60.3	54.9	32.1	49.9	53.1
K <sub>2</sub> O	1.26	1.35	0.70	34.6	5.95	3.18
CaO	6.24	4.78	3.81	20.3	22.0	10.2
Fe <sub>2</sub> O <sub>3</sub>	17.0	16.2	15.0	5.93	10.3	10.2
Al <sub>2</sub> O <sub>3</sub>	14.0	15.0	12.0	-	-	10.0
TiO <sub>2</sub>	1.37	2.13	1.91	0.32	0.58	1.28
P <sub>2</sub> O <sub>5</sub>	-	-	-	3.8	8.21	3.9
Br	-	-	10.3	-	-	3.7

#### 4. Conclusions

XRD characterization shows the decreasing of particle size in bentonite-OPBA nanocomposite. SEM results presented particle size uniformity in Bentonite-OPBA nanocomposite. Meanwhile, the FTIR results showed an absorption peak indicating bonding to the nanocomposite, which was also confirmed by the XRF results. XRF results show the content of SiO<sub>2</sub> and Al<sub>2</sub>O<sub>3</sub> in the nanocomposite to be applied as a nanofiller.

#### Acknowledgments

This research was funded by the Directory of Research and Community Service, Deputy for Research Strengthening and Development of the Ministry of Research and Technology/National Research and Innovation Agency to finance basic higher education research (PDUPT). Fiscal Year 2021 No: 12 / E1 / KP. PTNBH/2021, March 8, 202.

#### References

- Abeywardena, S. B. Y., Perera, S., Nalin de Silva, K. M., & Tissera, N. P. (2017). A facile method to modify bentonite nanoclay with silane. *International Nano Letters*, 7(3), 237–241. <https://doi.org/10.1007/s40089-017-0214-2>
- Abdullah, C. K., Ismail, I., Nurul Fazita, M. R., Olaiya, N. G., Nasution, H., Oyekanmi, A. A., Nuryawan, A., & H. P. S., A. K. (2021). Properties and Interfacial Bonding Enhancement of Oil Palm Bio-Ash Nanoparticles Biocomposites. *Polymers*, 13(10), 1615. <https://doi.org/10.3390/polym13101615>
- Ahmadi, S. (2020). Thermo Mechanical behaviour of Phenol Novolac Resin and Unsaturated Polyester Toughened Epoxy using nano Bentonite and Silica Nanoparticles. *Advances in Applied NanoBio-Technologies*, 1(3), 77–83. [https://doi.org/10.47277/aanbt/1\(3\)83](https://doi.org/10.47277/aanbt/1(3)83)
- Akl, M. A., Youssef, A. M., & Al-Awadhi, M. M. (2013). Adsorption of acid dyes onto bentonite and surfactant-modified bentonite. *Journal of Analytical & Bioanalytical Techniques*. 4(4), 3-7. <https://doi.org/10.4172/2155-9872.1000174>
- Alexandre, M., & Dubois, P. (2000). Polymer-layered silicate nanocomposites: Preparation, properties and uses of a new class of materials. *Materials Science and Engineering R: Reports*, 28(1), 1–63. [https://doi.org/10.1016/S0927-796X\(00\)00012-7](https://doi.org/10.1016/S0927-796X(00)00012-7)
- Andrunik, M., & Bajda, T. (2019). Modification of bentonite with cationic and nonionic surfactants: *Structural and textural features*. *Materials*, 12(22), 3772. <https://doi.org/10.3390/ma12223772>
- Bukit, N., & Frida, E. (2013). The effect zeolite addition in natural rubber polypropylene composite on mechanical, structure, and thermal characteristics. *Makara Journal of Technology*, 17(3), 3. <https://doi.org/10.7454/mst.v17i3.2926>
- Bukit, N., Ginting, E. M., Hutagalung, E. A., Sidebang, E., Frida, E., & Bukit, B. F. (2019). Preparation and characterization of oil palm ash from boiler to nanoparticle. *Reviews on Advanced Materials Science*, 58(1), 195–200. <https://doi.org/10.1515/rams-2019-0023>
- Bukit, N., Ginting, E. M., Pardede, I. S., Frida, E., & Bukit, B. F. (2018). Mechanical properties of composite thermoplastic hdpe / natural rubber and palm oil boiler ash as a filler. *Journal of Physics: Conference Series*, 1120(1), 0–8. <https://doi.org/10.1088/1742-6596/1120/1/012003>
- Bukit, N., Ginting, E. M., Sidebang, E., Frida, E., & Bukit, B. F. (2020). Mechanical Properties of Natural Rubber Compounds with Oil palm boiler ash and Carbon Black as a Filler. *Journal of Physics: Conference Series*, 1428(1). <https://doi.org/10.1088/1742-6596/1428/1/012020>
- Chen, X., Wang, X., Lu, Z., Luo, H., Dong, L., Ji, Z., Xu, F., Huo, D., & Hou, C. (2020). Ultra-sensitive detection of Pb<sup>2+</sup> based on DNAzymes coupling with multi-cycle strand displacement amplification (M-SDA) and nano-graphene oxide. *Sensors and Actuators, B: Chemical*, 311, 127898. <https://doi.org/10.1016/j.snb.2020.127898>
- Dhawale, K. D., Thorat, N. M., & Patil, L. R. (2018). An efficient and green synthesis of imidazoles using natural organic acids as promoter under solvent-free condition. *Asian Journal of Chemistry*, 29(8), 1709-1712. <https://doi.org/10.14233/ajchem.2017.20553>
- Fisli, A., & Yusuf, S. (2007). *Synthesis of Magnetic Nanocomposite with Natural Base Material for Thorium Adsorbent*. *Indonesian Journal of Materials Science*. 11(2), 93-98.
- Ginting, E. M., Bukit, N., Frida, E., & Bukit, B. F. (2020). Microstructure and thermal properties of natural rubber compound with palm oil boilers ash for nanoparticle filler. *Case Studies in Thermal Engineering*, 17, 100575. <https://doi.org/10.1016/j.csite.2019.100575>

- Ginting, E. M., Bukit, N., Motlan, Saragih, M. T., Frida, E., & Bukit, B. F. (2020). Analysis of natural rubber compounds with filler of Oil Palm Empty Bunches Powder and Carbon Black. *Journal of Physics: Conference Series*, 1428(1).  
<https://doi.org/10.1088/1742-6596/1428/1/012024>
- Ginting, E. M., Bukit, N., & Frida, E. (2017). Mechanical properties and morphology natural rubber blend with bentonite and carbon black. In *IOP Conference Series: Materials Science and Engineering*, 223 (1), 012003.  
<https://doi.org/10.1088/1757-899X/223/1/012003>
- Ginting, E. M., Motlan, Bukit, N., Saragih, M. T., Sinaga, A. H., & Frida, E. (2018). Preparation and Characterization of Oil Palm Empty Bunches Powder. *Journal of Physics: Conference Series*, 1120(1).  
<https://doi.org/10.1088/1742-6596/1120/1/012004>
- Hamada, H. M., Jokhio, G. A., Yahaya, F. M., Humada, A. M., & Gul, Y. (2018). The present state of the use of palm oil fuel ash (POFA) in concrete. *Construction and Building Materials*, 175, 26–40.  
<https://doi.org/10.1016/j.conbuildmat.2018.03.227>
- Ibrahim, S. M., & Abd Ali, Z. T. (2020). Using of modified-bentonite as low-cost sorbent for removal of methylene blue dye from aqueous solution. *Association of Arab Universities. Journal of Engineering Sciences*, 27(2), 45–54.  
<https://doi.org/10.33261/jaaru.2020.27.2.005>
- Ismail, H., Khoon, T. B., Hayeemasae, N., & Husseinsyah, S. (2015). Effect of oil palm ash on the properties of polypropylene/recycled natural rubber gloves/oil palm ash composites. *BioResources*, 10(1), 1495–1505.  
<https://doi.org/10.15376/biores.10.1.1495-1505>
- Jenita Rani, G., Jothi Rajan, M. A., & Gnana kumar, G. (2017). Reduced graphene oxide/ZnFe<sub>2</sub>O<sub>4</sub> nanocomposite as an efficient catalyst for the photocatalytic degradation of methylene blue dye. *Research on Chemical Intermediates*, 43(4), 2669–2690.  
<https://doi.org/10.1007/s11164-016-2788-0>
- Justice Babu, K., Sheet, S., Lee, Y. S., & Gnana Kumar, G. (2018). Three-Dimensional Dendrite Cu-Co/Reduced Graphene Oxide Architectures on a Disposable Pencil Graphite Electrode as an Electrochemical Sensor for Nonenzymatic Glucose Detection. *ACS Sustainable Chemistry and Engineering*, 6(2), 1909–1918.  
<https://doi.org/10.1021/acssuschemeng.7b03314>
- Karnati, S. R., Agbo, P., & Zhang, L. (2020). Applications of silica nanoparticles in glass/carbon fiber-reinforced epoxy nanocomposite. *Composites Communications*, 17, 32–41.  
<https://doi.org/10.1016/j.coco.2019.11.003>
- Legarto, C. M., Scian, A., & Lombardi, M. B. (2019). Preparation and characterization of bentonite nanocomposites via sol-gel process. *SN Applied Sciences*, 1(7), 1–7.  
<https://doi.org/10.1007/s42452-019-0801-0>
- Liang, X., Chen, X., Li, Z., Li, G., Chen, J., Yang, L., Shen, K., Xu, Y., & Mai, Y. (2019). Effect of deposition pressure on the properties of magnetron sputtering-deposited Sb<sub>2</sub>Se<sub>3</sub> thin-film solar cells. *Applied Physics A: Materials Science and Processing*, 125(6), 1–7.  
<https://doi.org/10.1007/s00339-019-2677-7>
- Majid, M. S. A., Ridzuan, M. J. M., & Lim, K. H. (2020). Effect of nanoclay filler on mechanical and morphological properties of Napier/ epoxy composites. *Interfaces in Particle and Fibre Reinforced Composites*, 137–162.  
<https://doi.org/10.1016/B978-0-08-102665-6.00006-6>
- My Linh, N. le, Duong, T., van Duc, H., Thi Anh Thu, N., Khac Lieu, P., van Hung, N., Hoa, L. T., & Quang Khieu, D. (2020). Phenol Red Adsorption from Aqueous Solution on the Modified Bentonite. *Journal of Chemistry*, 2020.  
<https://doi.org/10.1155/2020/1504805>
- Ogunlaja, S. B., & Pal, R. (2020). Effects of Bentonite Nanoclay and Cetyltrimethyl Ammonium Bromide Modified Bentonite Nanoclay on Phase Inversion of Water-in-Oil Emulsions. *Colloids and Interfaces*, 4(1), 2.  
<https://doi.org/10.3390/colloids4010002>
- Rabiatul, S., Islam, U., Alauddin, N., Sutarno, S., Mada, U. G., Suyanta, S., & Mada, U. G. (2020). Indonesian Journal of Chemical Research Adsorption-Desorption Studies of Phosphate on CTAB Modified Bentonite Indonesian. *Journal of Chemical Research*.
- Rihayat, T., Riskina, S., & Syahputra, W. (2019, June). Formulation of Polyurethane with Bentonite-Chitosan as Filler Applied to Carbon Steel as an Antibacterial and Environmentally Friendly Paint. In *IOP Conference Series: Materials Science and Engineering*, 536 (1), 012093.  
<https://doi.org/10.1088/1757-899X/536/1/012093>
- Saba, N., Md. Tahir, P., Abdan, K., & Ibrahim, N. A. (2015). Preparation and characterization of fire-retardant nano-filler from oil palm empty fruit bunch fibers. *BioResources*, 10(3), 4530–4543.  
<https://doi.org/10.15376/biores.10.3.4530-4543>

- Schampera, B., Šolc, R., Tunega, D., & Dultz, S. (2016). Experimental and molecular dynamics study on anion diffusion in organically modified bentonite. *Applied Clay Science*, 120, 91–100.  
<https://doi.org/10.1016/j.clay.2015.11.026>
- Shakir, S., Saravanan, J., Rizan, N., Jusice Babu, K., Aziz, M. A., Moi, P. S., Periasamy, V., & Gnana kumar, G. (2018). Fabrication of capillary force induced DNA template Ag nanopatterns for sensitive and selective enzyme-free glucose sensors. *Sensors and Actuators, B: Chemical*, 256, 820–827.  
<https://doi.org/10.1016/j.snb.2017.10.021>
- Sirait, M., Bukit, N., & Siregar, N. (2017, January). Preparation and characterization of natural bentonite into nanoparticles by co-precipitation method. In AIP conference proceedings, 1801 (1), 020006.  
<https://doi.org/10.1063/1.4973084>
- Sirait, M., Gea, S., Bukit, N., Siregar, N., & Sitorus, C. (2018). Synthesis of nanobentonite as heavy metal adsorbent with various solvents. *Oriental Journal of Chemistry*, 34(4), 1854–1857.  
<https://doi.org/10.13005/ojc/3404020>
- Siva, G., Aziz, M. A., & Gnana Kumar, G. (2018). Engineered Tubular Nanocomposite Electrocatalysts Based on CuS for High-Performance, Durable Glucose Fuel Cells and Their Stack. *ACS Sustainable Chemistry and Engineering*, 6(5), 5929–5939.  
<https://doi.org/10.1021/acssuschemeng.7b04326>
- Van Jaarsveld, J. G. S., Van Deventer, J. S. J., & Lukey, G. C. (2003). The characterisation of source materials in fly ash-based geopolymers. *Materials Letters*, 57(7), 1272–1280.  
[https://doi.org/10.1016/s0140-6701\(04\)91393-8](https://doi.org/10.1016/s0140-6701(04)91393-8)
- Wang, Q., Rhimi, B., Wang, H., & Wang, C. (2020). Efficient photocatalytic degradation of gaseous toluene over F-doped TiO<sub>2</sub>/exfoliated bentonite. *Applied Surface Science*, 530, 1–12.  
<https://doi.org/10.1016/j.apsusc.2020.147286>
- Wang, X., Yang, L., Zhang, J., Wang, C., & Li, Q. (2014). Preparation and characterization of chitosan–poly(vinyl alcohol)/bentonite nanocomposites for adsorption of Hg(II) ions. *Chemical Engineering Journal*, 251, 404–412.  
<https://doi.org/10.1016/J.CEJ.2014.04.089>
- Yu, L., Wang, D., Tan, Y., Du, J., Xiao, Z., Wu, R., ... & Huang, J. (2018). Super tough bentonite/SiO<sub>2</sub>-based dual nanocomposite hydrogels using silane as both an intercalator and a crosslinker. *Applied Clay Science*, 156, 53–60.  
<https://doi.org/10.1016/j.clay.2018.01.026>
- Yuzhen, L., Huang, Z., Xia, Y., Shi, J., & Gao, L. (2020). Adsorption equilibrium, isotherm, kinetics, and thermodynamic of modified bentonite for removing Rhodamine B. *Indian Journal of Chemical Technology (IJCT)*. 27(2), 116–125.
- Zarina, Y., Mustafa Al Bakri, A. M., Kamarudin, H., Nizar, I. K., & Rafiza, A. R. (2013). Review on the various ash from palm oil waste as geopolymer material. In *Reviews on Advanced Materials Science*, 34(1), 37–43.